Competitive regulation of CaT-like-mediated Ca^{2+} entry by protein kinase C and calmodulin

Barbara A. Niemeyer, Christiane Bergs, Ulrich Wissenbach, Veit Flockerzi*, and Claudia Trost

Institut für Pharmakologie und Toxikologie der Universität des Saarlandes, 66421 Homburg, Germany

Edited by Lutz Birnbaumer, University of California, Los Angeles, CA, and approved January 5, 2001 (received for review October 26, 2000)

A finely tuned Ca^{2+} signaling system is essential for cells to transduce extracellular stimuli, to regulate growth, and to differentiate. We have recently cloned CaT-like (CaT-L), a highly selective Ca^{2+} channel closely related to the epithelial calcium channels (ECaC) and the calcium transport protein CaT1. CaT-L is expressed in selected exocrine tissues, and its expression also strikingly correlates with the malignancy of prostate cancer. The expression pattern and selective Ca^{2+} permeation properties suggest an important function in Ca^{2+} uptake and a role in tumor progression, but not much is known about the regulation of this subfamily of ion channels. We now demonstrate a biochemical and functional mechanism by which cells can control CaT-L activity. CaT-L is regulated by means of a unique calmodulin binding site, which, at the same time, is a target for protein kinase C-dependent phosphorylation. We show that Ca^{2+}-dependent calmodulin binding to CaT-L, which facilitates channel inactivation, can be counteracted by protein kinase C-mediated phosphorylation of the calmodulin binding site.

Tight regulation of intracellular Ca^{2+} homeostasis is essential for the survival of virtually all cell types. Although much is known about the components and their physiological function maintaining rapid Ca^{2+} signaling in excitable tissue (1, 2), less is known in nonexcitable cells. Although there is growing evidence for changes in Ca^{2+}-homeostasis causing cells to proliferate and ultimately become malignant cancer cells (3), the molecular components that cause these changes are largely unknown. A subfamily of Ca^{2+}-selective ion channels has recently emerged that is involved in transcellular Ca^{2+} uptake in epithelial cells (4, 5), and its members are very distantly related to transient receptor potential (TRP)-channels. In contrast to the activation mechanism discussed for some of the classic members of the mammalian TRP family (6, 7), these epithelial channels are not likely to be gated by depletion of internal calcium stores (5, 8). We have recently identified a member of this family, human calcium transport protein-like (CaT-L), and demonstrated that its physiological profile concerning current size and Ca^{2+} selectivity resembles that of rabbit epithelial calcium channels (ECaC) (9). Its sequence is almost identical to the also recently cloned human CaT1 (10), but its expression pattern in healthy trophoblasts and syncytiotrophoblasts of the placenta, pancreatic acinar cells, and salivary glands, but not in kidney or small intestine differs from rabbit ECaC and rat CaT1 beyond the expected species differences. Interestingly, we found that, whereas CaT-L expression cannot be detected in normal prostate tissues, its expression increases when these tissues undergo malignant transformation to metastatic stages that infiltrate the rest of the body (9).

The expression pattern and the selective Ca^{2+} permeation properties of CaT-L channels suggest an important function in Ca^{2+} uptake and possibly in the potential for cellular transformation. The regulation and modulation of the related ECaC are not well characterized, and, given the fact that CaT-L shows very low overall homology (13–19% sequence identity) to the better characterized members of the "classic" TRP family, such as *Drosophila* TRP and TRPL (for review see refs. 11–13), we investigated feedback regulation of CaT-L channel activity. We show that inactivation of CaT-L is a multiphasic process with a rapid calcium-dependent phase and a later calcium-calmodulin (Ca^{2+}-CaM)-dependent phase. We further demonstrate by biochemical and functional analyses that the calmodulin-dependent inactivation can be counteracted by phosphorylation through protein kinase C (PKC).

Materials and Methods

Site-Directed Mutagenesis. To obtain the short CaT-L variant (S), two complementary oligonucleotides that introduced two stop codons after a *Mun*I recognition site and contained a 3′ *Nhe*I recognition site were ligated into the *Mun*I/*Nhe*I-digested pdiCaT-L plasmid (9), yielding truncated CaT-L (CaT-L Δ 693–725). To obtain the 6 R/E mutant, amino acid changes were introduced by using mutated oligonucleotides (R697/E, R699/E, R704/G, R705E, R708/E, R713/E) and wild-type CaT-L as template. Resulting PCR fragments were subcloned into the *Mun*I/*Nhe*I-digested pdiCaT-L and pcDNA3 vectors and sequenced. *In vitro* transcription and translation of CaT-L and mutant constructs was performed by using the TnT7 Quick translation kit (Promega). *In vitro* translated proteins were isolated by gel filtration with Sephadex G50 columns. Chinese hamster ovary (CHO) cells were transfected with pdiCaT-L and with mutant constructs as described (9). To obtain the FLAG-tagged CaT-L construct, we inserted an *Eco*RV-digested FLAG epitope (DYKDDDDK) in the *Eco*RV recognition site at amino acid position 383 of CaT-L. Sequencing revealed a tandem insertion of four FLAG epitopes at this position.

Electrophysiology. Patch-clamp recordings on single transfected CHO cells were performed 1 day after transfection as described (9). Pipette solution contained (in mM): 140 aspartic acid, 10 EGTA, 10 NaCl, 1 $MgCl_2$, 10 Hepes (pH 7.2 with CsOH). Bath solution contained (in mM): 100 NaCl, 10 CsCl, 2 $MgCl_2$, 50 mannitol, 10 glucose, 20 Hepes (pH 7.4 with CsOH) and 30 $CaCl_2$, or 30 $BaCl_2$. After break-in, whole cell currents were recorded every 10 s by applying 100-ms voltage-clamp ramps from −100 mV to +100 mV from a holding potential of +70 mV until ramp currents reached steady state. Twenty seconds after reaching steady state, a 1-s voltage step to −100 mV was applied. Data are given as mean ± SEM. Values were not corrected for liquid junction potentials. PKC inhibitors bisindolylmaleimide I and Gö6983 and the phorbol ester PMA (phorbol 12-myristate 13-acetate) were from Calbiochem.

Glutathione *S*-Transferase (GST)-CaT-L Fusion Proteins and Pull-Down Assays. CaT-L sequences were amplified by PCR, subcloned into pGEX-KG, sequenced, and expressed in *Escherichia coli* BL21.

This paper was submitted directly (Track II) to the PNAS office.

Abbreviations: CaT-L, calcium transport protein-like; ECaC, epithelial calcium channel; Ca^{2+}-CaM, calcium-calmodulin; PKC, protein kinase C; S, short CaT-L variant; PMA, phorbol 12-myristate 13-actate; GST, glutathione *S*-transferase.

*To whom reprint requests should be addressed. E-mail: veit.flockerzi@med-rz.uni-sb.de.

The publication costs of this article were defrayed in part by page charge payment. This article must therefore be hereby marked "*advertisement*" in accordance with 18 U.S.C. §1734 solely to indicate this fact.

www.pnas.org/cgi/doi/10.1073/pnas.051511398

CaM-agarose or GST-CaT-L fusion proteins bound to glutathione-Sepharose were equilibrated in TBS buffer containing 0.1% Triton X-100 and 1 mM $CaCl_2$ or 2 mM EGTA. Incubation with *in vitro*-translated [^{35}S]CaT-L protein or [^{35}S]CaM was followed by three washes with the appropriate buffers, and bound proteins were eluted with sample buffer, subjected to SDS gel-electrophoresis, and exposed to phosphoimager (Fuji BAS 2500) screens.

Overlay and Ca^{2+} Dependency. GST-C1 fusion protein was run on SDS/PAGE gels and blotted on nitrocellulose, blocked in 140 mM KCl, 20 mM Hepes, 10 mM EGTA, 0.1% Triton X-100, pH 7.2 (KHE), with 5% milk-powder for 30 min and washed 3 × 10 min in above solution without blocking agent. Blots were cut into strips containing ≈2 μg C1 fusion protein each and incubated with 600,000 cpm of [^{35}S]CaM in the absence and presence of different [Ca^{2+}] for 3 h at 21°C. Free [Ca^{2+}] was adjusted by using appropriate chelators (EGTA, HEDTA, NTA) and $CaCl_2$ according to the SLIDERS V. 2.00 software (http://www.stanford.edu/~cpatton/maxc.html). Membranes were washed for 3 × 10 min in the corresponding binding buffers to remove unbound CaM. After drying and autoradiography, the relative intensities of the bands were analyzed by using AIDA software (Raytest, Straubenhardt, Germany).

Fluorometric Measurements with Dansyl-CaM. Dansyl-CaM was synthesized according to ref. 14, purified by centrifugation with Vivaspin 5000 concentrators, and washed three times with 20 mM NH_4HCO_3 (pH 7.4). Measurement of absorbance at 340 nm (molar extinction coefficient: 3400 M^{-1} cm^{-1}) showed incorporation of 1.1 mol dansyl/mol CaM. Fluorescence emission spectra were monitored at 20°C on a luminescence spectrometer (Perkin–Elmer LS50) in the presence of 20 mM Hepes, pH 7.4, 200–400 nM dansyl-CaM, and different concentrations of peptides and 1 mM $CaCl_2$ or 2 mM EGTA. The excitation wavelength was 340 nm, slit width was 5 nm, and emission wavelengths between 400 and 600 nm were measured. The fractional degree of saturated dansyl-calmodulin fluorescence (a) was calculated as $a = (F - F_0)/(F_\infty - F_0)$, where F_∞ represents the fluorescence intensity at saturated peptide levels. a was plotted as a function of free peptide concentrations, and the dissociation constants for the CaM-peptide binding were calculated from curve fitting by using SIGMAPLOT 4.0 software.

Phosphorylation Assay with PKC-α. The synthetic peptide 395 was phosphorylated with PKC-α (Calbiochem) in a buffer containing 20 mM Tris·HCl, pH 7.5, 5 mM $MgCl_2$, 0.2 mM $CaCl_2$, 5 μM [γ-^{32}P]ATP (specific activity 10,000 cpm/pmol ATP), 100 μg/ml L-α-phosphatidyl-L-serine, 100 ng/ml PMA in the absence or presence of CaM (bovine brain; Calbiochem) in a final volume of 20 μl. The reaction was started by addition of 2 nM protein kinase Cα. After incubation for 3 min at 30°C, the reaction was stopped by spotting the mix onto P-81 paper followed by three 5-min washes in 75 mM H_3PO_4, and incorporated ^{32}P was counted by Cerenkov radiation. Phosphorylation of CAT-L-C3 GST fusion protein (3 pmol) was performed as described above, and the reaction was stopped after 2, 5, 10, 15, 30, 60, and 90 min by addition of sample buffer. Incorporated ^{32}P was analyzed after SDS/PAGE electrophoresis by phosphoimager analysis. To study phosphorylation study of the full-length channel protein, CaT-L including the FLAG-epitope was expressed in HEK cells (≈50,000 cells before transfection), harvested 24 h after transfection, and membrane proteins were solubilized in 50 mM Tris·HCl, pH 7.5, 150 mM NaCl, 2.5% polyoxyethylene 9 lauryl ether (Lubrol) with a mixture of protease inhibitors, and tagged proteins were purified by using anti-FLAG M2-agarose (Sigma). Phosphorylation of CAT-L was performed as described above by using ≈1/50 volume of the anti-FLAG-agarose eluate and 4 nM PKC for 20 min at 37°C in 80 μl. Reaction was stopped by addition of sample buffer.

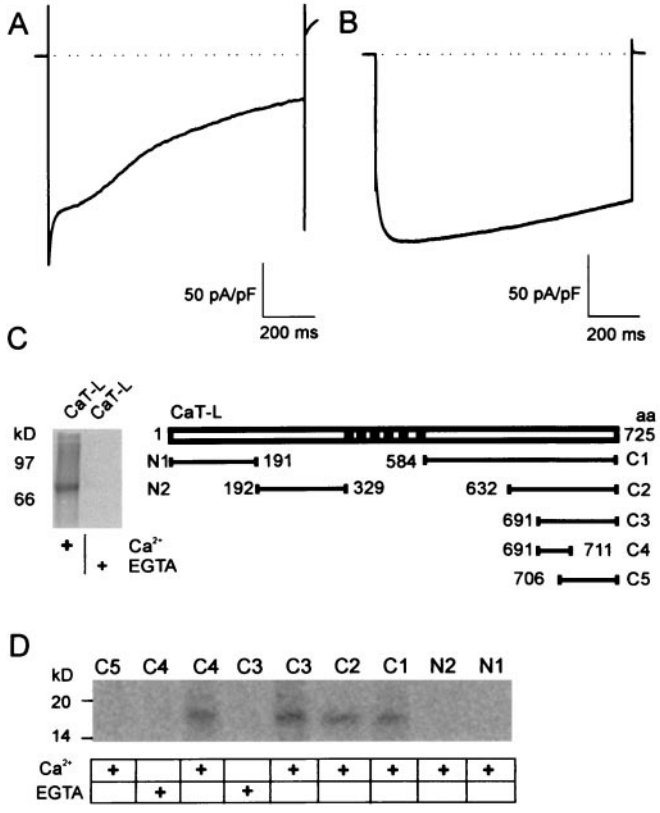

Fig. 1. CaT-L. shows Ca^{2+}-dependent inactivation and binds calmodulin. (*A*) Representative current recorded during a voltage step to −100 mV. At least two inactivation time constants can be distinguished in 30 mM $[Ca^{2+}]_o$. (*B*) Current recorded in 30 mM $[Ba^{2+}]_o$. Note that activation is delayed, the initial fast inactivation component is missing, and currents only show a very slow second component of inactivation. (*C*) ^{35}S-labeled CaT-L binds to CaM-agarose in the presence, but not absence of Ca^{2+} (*Left*). GST-fusion proteins of CaT-L were constructed according to the schematic drawing (*Right*). aa, amino acid residues. (*D*) Binding of [^{35}S]CaM to different CaT-L GST-fusion proteins in the presence (+) or absence of calcium.

Results

In our initial paper describing the cloning and expression of CaT-L (9), we found that, when expressed in different cell lines, CaT-L forms constituitively open ion channels that show an inwardly rectifying current-voltage relationship with a high selectivity of calcium over monovalent cations. Their activity is correlated with the electrochemical driving force for Ca^{2+} and the level of intracellular Ca^{2+} ($[Ca^{2+}]_i$), suggesting that calcium-dependent regulatory mechanisms exist. To investigate this further, we recorded CaT-L-mediated Ca^{2+} currents in response to a hyperpolarizing voltage step (Fig. 1*A*), which then show a strong time-dependent inactivation with at least two different kinetic components. This inactivation behavior is largely mediated by calcium as substitution of calcium by barium alters activation and inactivation: rapid and multiphasic inactivation is abolished, although I_{Ba} still inactivates very slowly (Fig. 1*B*). Although the time course of the initial rapid inactivation suggests a negative feedback mechanism with little delay, possibly by Ca^{2+} itself, the difference between the overall inactivation between Ca^{2+}- and Ba^{2+}-mediated currents of the later phase may indicate the involvement of additional Ca^{2+}-dependent factors with slower kinetics. One protein known to be involved

PHYSIOLOGY

in feedback regulation of many ion channels is CaM (for review see ref. 15). We thus first examined whether the entire ^{35}S-labeled *in vitro*-translated CaT-L protein can bind to CaM agarose in a Ca^{2+}-dependent manner. As shown in Fig. 1*C*, the ≈83-kDa CaT-L protein binds to CaM in the presence, but not in the absence, of Ca^{2+}. To identify CaM binding sites, GST-fusion proteins encompassing different N- and C-terminal CaT-L domains (Fig. 1*C*) were constructed and expressed in *E. coli*. Approximately 2 μg of each fusion protein bound to glutathione-Sepharose was incubated with [^{35}S]CaM in the presence of 1 mM Ca^{2+} or 2 mM EGTA. The CaM binding site is located within the C-terminal domain of CaT-L (C1 fusion protein, Fig. 1*D*). Several smaller fusion proteins were then constructed and tested. Fusion protein C4 encompassing amino acid residues 691–711 was found to be sufficient to bind CaM (Fig. 1*D*). Alignment of the CaT-L-CaM binding site with corresponding domains of closely related proteins, namely CaT1 and ECaC, suggests that a similar CaM binding site exists in CaT1, whereas ECaC shows a less conserved site and may bind CaM with a different affinity. The site also conforms with structural predictions for CaM binding sites by forming an amphiphilic α-helix (16) (Fig. 2*A*).

To estimate the stoichiometry and affinity of Ca^{2+}-CaM binding to CaT-L, we measured the binding of dansyl-CaM to the synthetic peptide 395 encompassing amino acid residues 694–716 (Fig. 2*A*). When dansyl-CaM interacts with peptide 395 in the presence of 1 mM Ca^{2+}, the dansyl-CaM emission spectra displays a characteristic shift in the absorption of blue light and an increase in fluorescence intensity. As shown in Fig. 2*C*, fluorescence intensity of 200 nM dansyl-CaM increased almost linearly with increasing peptide concentration and reached a plateau at ≈0.2 μM, thus confirming a 1:1 stoichiometry between CaT-L peptide and CaM. The apparent dissociation constant (K_d) of ≈65 nM conforms with other CaM substrates. A similar K_d was obtained at 100 μM Ca^{2+} (data not shown).

As the cellular CaM concentration is in the order of several μM, exceeding the K_d value of the CaT-L binding site, occupation of the site *in vivo* should only depend on variations of the cytosolic Ca^{2+} concentration. To determine the Ca^{2+} dependency of CaM binding, [^{35}S]CaM was bound to blotted CaT-L fusion protein in the absence and presence of increasing [Ca^{2+}]. After washes with the respective buffers (see *Materials and Methods*), blots were exposed to phosphoimager screens. Fig. 2*D* shows one representative experiment (*Upper*). The intensity of bands indicating the amount of bound [^{35}S]CaM were analyzed, and the averaged data of four experiments were plotted against the [Ca^{2+}]. At a [Ca^{2+}] of ≈7.4 μM, 50% of the CaT-L binding site is occupied by Ca^{2+}-CaM. Quite consistently, we noticed a partial decrease of binding affinity in the overlay assay at [Ca^{2+}] ≥ 100 μM, which might reflect direct interference of Ca^{2+} with Ca^{2+}-CaM binding to CaT-L.

Analyzing the amino acid sequence of the CaM binding site, we recognized a consensus sequence for a PKC phosphorylation site (RQG*T*LRR, see arrow in Fig. 2*A*). Alignment of the CaT-L CaM binding domain with an optimal PKC-α-phosphorylation recognition domain and its pseudosubstrate (psd) domain (17) predicts that the CaT-L-CaM binding domain is most likely an excellent substrate for PKC (Fig. 3*A*). Phosphorylation at the target threonine adds negative charges to the helix, and, therefore, binding of CaM might be influenced. We first tested this hypothesis by adding peptide 396 (amino acids 649–716), phosphorylated at threonine 702, to dansyl-CaM and recorded changes of the dansyl-CaM fluorescence. As shown in Fig. 3*B*, no change in fluorescence intensity, i.e., binding of the peptide to the dansyl-CaM, could be observed, indicating that CaM cannot bind to the phosphorylated peptide. To test whether peptide 395 can be phosphorylated at T702 *in vitro*, we performed phosphorylation assays by using the ubiquitously expressed PKC-α

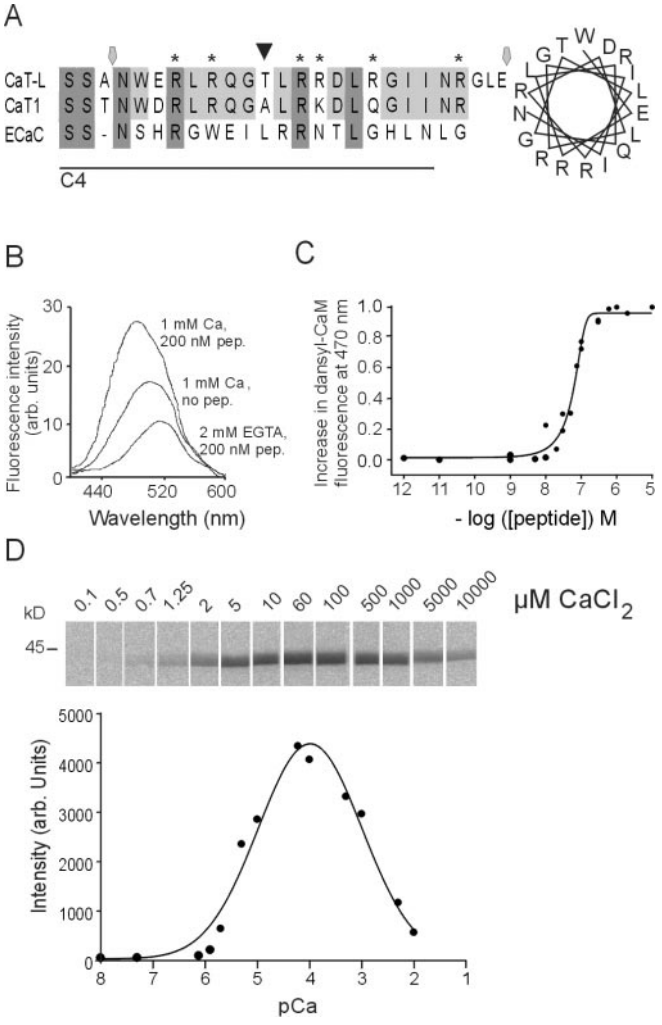

Fig. 2. Properties of CaT-L's CaM binding site. (*A*) Sequence of the CaM binding site and corresponding regions of CaT1 (no. AAD47636) and ECaC (no. CAB40138). Line shows C4 fusion protein, hexagonal markers indicate peptide 395, and arrow points to a PKC phosphorylation site in CaT-L. Helical wheel representation of the CaM binding site (*Right*). (*B*) Dansyl-CaM fluorescence spectra in the absence or presence of 200 nM CaT-L peptide 395 at 1 mM Ca^{2+} or 2 mM EGTA. (*C*) Fluorescence as a function of free peptide concentration. Data points show the average of two to four experiments and the apparent K_d was 65 nM. (*D*) Overlay blot of GST-CaT-L C1 protein incubated with [^{35}S]CaM at different [Ca^{2+}] (*Upper*) with the mean amount of bound CaM measured by densiometric analyses as a function of free [Ca^{2+}] (n = 4; *Lower*).

isoform (Fig. 3*C*). PKC-α readily phosphorylates peptide 395 with apparent V_{max} and K_m values of 1.36 ± 0.25 μmol/mg/min and 2.97 ± 0.84 μM (n = 3). These values correlate well with values described for other PKC substrates (18, 19). If PKC competes with CaM for access to the CaT-L peptide, we would expect to see a decrease of phosphorylation in the presence of excess CaM. We therefore tested phosphorylation of peptide 395 in the presence of increasing CaM concentrations (Fig. 3*C*). Preincubation of 0.1–4 μM peptide with 20 μM CaM completely prevented phosphorylation of the peptide, whereas, at higher peptide or lower CaM concentrations, PKC had access to the phosphorylation site and phosphorylated the peptide. To test whether the native full-length channel protein can become phosphorylated, we expressed CaT-L tagged with the FLAG-epitope in HEK cells, isolated CaT-L by its binding to FLAG agarose, and showed that the retained protein is phosphorylated (Fig. 3*D*, *Left*). CaT-L protein contains several predicted PKC

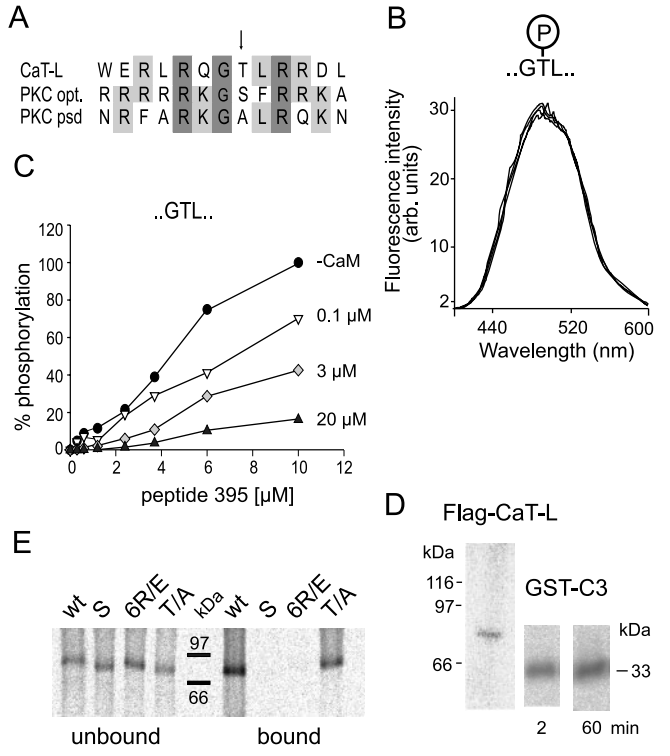

Fig. 3. Influence of phosphorylation on CaM binding to CaT-L. (*A*) Alignment of CaT-L's CaM binding site with PKC-α's optimal binding site (opt.) and pseudosubstrate domain (psd). (*B*) Fluorescence spectra of dansyl-CaM in the absence and presence of 0, 0.2, 0.4, and 1 μM phosphorylated CaT-L peptide 396. (*C*) Relative increase in phosphorylation of peptide 395 as a function of peptide and increasing CaM concentration using 2 nM PKC-α. (*D*) Autoradiographs showing phosphorylation of CaT-L protein tagged with the FLAG-epitope (*Left*) and of GST-C3 protein by PKC-α (*Right*). (*E*) CaM-agarose pull-down assay using wild-type and mutated CaT-L.

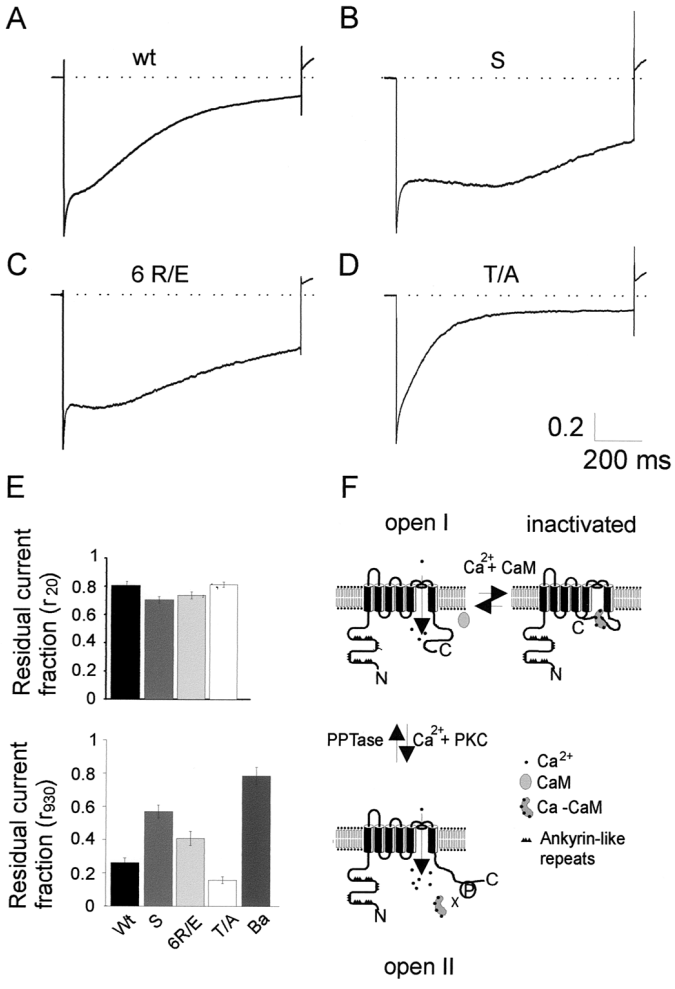

Fig. 4. Physiological consequence of Ca^{2+}-CaM binding to CaT-L. Normalized (I/I_{max}) current traces in response to a voltage step to −100 mV for wild-type (*A*), CaM binding site deletion construct S (*B*), point mutant construct 6 R/E (*C*), and disabled phosphorylation site mutant T/A (*D*). Note the different inactivation profiles. (*E*) Quantification of the residual current fraction within the first 20 ms (r20) and within the next 930 ms (r930). In the case of barium as charge carrier, residual current fraction (r930) was calculated from peak to t = 930. (*F*) Model of CaT-L regulation by PKC and Ca^{2+}-CaM.

phosphorylation sites (9) and thus may not be phosphorylated at T702 only. We therefore phosphorylated GST-CaT-L fusion protein C3 (see Fig. 1*C*), which only contains the T702 site. As seen in Fig. 3*D Right*, phosphorylation of C3 is almost complete after 2 min, indicating that T702 of CaT-L is an excellent substrate for PKC-dependent phosphorylation. These findings suggest that phosphorylation of CaT-L and Ca^{2+}-dependent CaM binding are likely to play a role in channel regulation *in vivo*.

To characterize this regulation *in vivo*, we first altered the CaM binding site and tested the ability of *in vitro*-translated CaT-L mutants to bind CaM in the presence of 60 μM free Ca^{2+}. Three mutants were constructed, the first by deleting the last 32 amino acid residues of CaT-L's C terminus containing the entire CaM binding site (S, short construct), and the second by mutating six arginine residues within the CaM binding site (see asterisks in Fig. 2*A*) to five oppositely charged glutamate residues and one glycine residue (named 6 R/E). In the third mutant, we changed the PKC substrate threonine (T702) to an alanine residue (T/A), as pointed out by the arrow in Figs. 2*A* and 3*A*. The single point mutation should not affect CaM binding but abolish phosphorylation by PKC. As predicted, after *in vitro* translation and ^{35}S-labeling of the different constructs, no binding to CaM-agarose was observed for the truncated channel (S) and the point mutant (6 R/E), whereas CaT-L wild-type and the (T/A) mutant bound to Ca^{2+}-CaM (Fig. 3*E*).

We then transiently expressed wild-type and mutated channel constructs and performed whole-cell patch-clamp recordings (Fig. 4). All three CaT-L mutants gave rise to normal ramp currents reversing at >+50 mV (data not shown). If CaM binding is important for channel inactivation, one would expect to see an altered inactivation behavior in mutants that do not bind CaM. Fig. 4 shows sample current traces of wild-type CaT-L (*A*), short mutant S (*B*), point mutant 6 R/E (*C*), and phosphorylation site mutant T/A (*D*) in response to a hyperpolarizing voltage pulse to −100 mV. Interestingly, neither mutant showed a slow-down in the initial fast phase of inactivation (≈20 ms after step to −100 mV) when compared with wild-type channels (Fig. 4*E Upper*). The most striking difference was observed in the next 400–500 ms of the pulse. During this time, mutant channels that do not bind CaM almost completely fail to inactivate, but proceed to inactivate afterward. To quantitate this multiphasic inactivation behavior, we measured the current size 2 ms after peak—to avoid possible capacitance artefacts—and 20 ms later and calculated the residual current fraction (r_{20}). Slow inactivation was calculated as the residual current fraction (r_{930}) of the subsequent 930 ms (Fig. 4*E*). Although no delay in inactivation could be observed for any of the mutant constructs within the first 20 ms of the pulse (Fig. 4*E Upper*), the residual

current fraction (r_{930}) was significantly larger (0.57 ± 0.039, $n = 13$) for S compared with wild-type (0.26 ± 0.03, $n = 14$; $P < 0.00001$). 6 R/E behaved similar to S and showed larger r_{930} values than wild-type (0.41 ± 0.044, $n = 13$; $P < 0.05$), although the difference was not as dramatic. Given the fact that CaT-L can be phosphorylated at its CaM binding site (see Fig. 3) and is then unable to bind Ca^{2+}-CaM, we wondered whether a fraction of the expressed wild-type channels is already phosphorylated. These channels would then be unable to bind Ca^{2+}-CaM and reduce the effect of disturbing Ca^{2+}-CaM binding. If this is the case, all of the expressed T/A mutant CaT-L channels, unable to become phosphorylated at their CaM-binding site, should be able to bind Ca^{2+}-CaM and show faster inactivation than wild-type channels. As shown in Fig. 4 *D* and *E*, this is indeed what we observed. The T/A mutant-mediated currents show faster inactivation kinetics than wild-type channels [r_{930} for T/A mutant ($n = 10$) was 0.16 ± 0.02 vs. 0.26 ± 0.03 for wt; $P < 0.01$], implicating that phosphorylation of the CaM binding site indeed alters the inactivation of CaT-L mediated currents *in vivo*. We also recorded the inactivation behavior of all genotypes with 30 mM Ba^{2+} as charge carrier and obtained the following results for the inactivation behavior (I_{930}/I_{max}) $\pm$ SEM: wt: 0.73 ± 0.04 ($n = 10$); 6 R/E: 0.78 ± 0.03 ($n = 5$); S: 0.74 ± 0.04 ($n = 6$); T/A: 0.67 ± 0.06 ($n = 10$). Neither of these inactivation profiles are significantly different from each other. We have also checked the shape of the I/V curves, current densities, and reversal potentials for all genotypes and found no difference between wild-type and mutants, which also confirms that we have not changed the biophysical channel properties other than altering their calcium dependent inactivation mechanism. We have furthermore conducted experiments to test the influence of inhibition and stimulation of PKC on wild-type channels *in vivo*. To inhibit PKC activity, we have used a mix of the specific PKC blockers Bisindolylmaleimide I and Gö6983 at 1 μM concentration. To stimulate, we added 100 nM of the phorbol ester PMA to the bath. We obtained the following results for the r_{930} values $\pm$ SEM : wild-type 0.26 ± 0.03 ($n = 14$, see initial result); wild-type with inhibitors added: 0.21 ± 0.03 ($n = 6$); and wild-type with PMA added: 0.31 ± 0.06 ($n = 8$). Addition of either drug showed effects in the expected direction, namely a speed-up if phosphorylation is prevented and a slow down if phosphorylation is encouraged; however, neither result is statistically significant different from wild type. Considering that our current measurements are done in an "*in vivo*," but heterologous overexpression system where basal Ca^{2+} levels are raised because of channel expression (9) and may influence PKC activation and CaM binding in the resting state, expression of the mutant constructs can be expected to yield clearer results compared with the pharmacological experiments.

Discussion

Our experiments revealed exciting features of CaT-L, a Ca^{2+}-selective channel that is distantly related to the TRP family of ion channels. Very little is known about the regulation of CaT-L or of the most closely related epithelial calcium channels in respect to calcium binding proteins, such as calmodulin or other second messengers. Calmodulin is a ubiquitous protein known to regulate the activity of different ion channels, Ca^{2+} pumps and other proteins in a Ca^{2+}-dependent manner (for review, see refs. 15 and 20). At rest, when Ca^{2+} concentrations are low, Ca^{2+} entry through L-type voltage-gated Ca^{2+} channels, cyclic nucleotide-gated channels, and *N*-methyl-D-aspartate receptors is enabled (21, 22) (for review, see ref. 15). On Ca^{2+} influx, activated Ca^{2+}-CaM inactivates the above mentioned influx pathways as well as Trpl-mediated currents in *Drosophila* photoreceptors (23), but activates potassium currents through the small- and intermediate-conductance Ca^{2+}-activated potassium channels (24, 25) that hyperpolarize cells and counteract Ca^{2+} entry.

Given CaT-L's selective expression in certain exocrine tissues and in malignant cancer cells of prostate origin, knowledge of the feedback mechanism may be critical for understanding function and differentiation in these cells. We showed that Ca^{2+} inactivates CaT-L channels in several ways: First, there is a rapid inactivation of CaT-L channels that is clearly independent of CaM binding and could be because of a local effect of Ca^{2+} on the intracellular pore forming region (see refs. 26 and 27 for ECaC), but was not investigated further. Secondly, there is a slower inactivation that was found to be Ca^{2+}-CaM dependent. Although CaM does not bind to CaT-L at [Ca^{2+}] normally present in cells at rest, binding was observed at increased [Ca^{2+}] with maximal binding at ≈ 60 μM Ca^{2+}. Ca^{2+}-CaM binding inactivates CaT-L channels, although additional Ca^{2+}-dependent and -independent inactivation or run-down mechanisms must still exist (Fig. 4): Removal of CaM binding does not affect the initial rapid phase of inactivation, nor does it abolish all of the slow inactivation. Binding of Ca^{2+}-CaM, however, can be prevented by PKC mediated phosphorylation of a threonine residue within the CaM binding site. Conversely, substitution of the target threonine leads to faster inactivation of CaT-L-mediated currents, as binding of Ca^{2+}-CaM cannot be prevented by phosphorylation (see Fig. 4*E*). This convergence on a shared substrate domain may represent an important mechanism to control the timing and convergence of signal responses (reviewed in ref. 28). Dual regulation of a calmodulin binding site by protein kinase A and partially by PKC has been postulated for *Drosophila* TRPL (29), although no functional data were included. Interestingly, CaT-L's closest relatives, the Ca^{2+} transporter CaT1 and the epithelial Ca^{2+} channel ECaC (4, 5, 8), are likely to be regulated at the corresponding region by CaM but lack the PKC phosphorylation site (see Fig. 3*A*). The Ca^{2+} requirement for activation of PKC depends on the PKC isoform (30) and can be either lower or higher than the Ca^{2+}-requirement for CaM binding. PKC activity thus may act as a switch that can regulate the amount of Ca^{2+}-influx through CaT-L channels by altering their inactivation behavior (Fig. 4*F*).

Our results suggest a model in which CaT-L-expressing cells can show a substantial Ca^{2+}-influx, where phosphorylation of CaT-L channels can act as a positive feedback system, delaying inactivation. Given our previous finding that CaT-L expression serves as a marker for prostate cancer, it is tempting to speculate that the finely tuned feedback mechanism that must exist in CaT-L-expressing exocrine cells (9) has gone astray in cancer cells. Here, increased activation of protein kinases (31) could lead to up-regulated Ca^{2+} influx through CaT-L channels and, as a consequence, altered Ca^{2+}-homeostasis and gene expression.

We thank Trisha Davis for kindly providing the CaM cDNA, Markus Hoth for comments on the manuscript, and Stephan Philipp for comments on the manuscript and for providing the pdi vector. This work was supported in part by the Deutsche Forschungsgemeinschaft and the Fonds der Chemischen Industrie.

1. Clapham, D. E. (1995) *Cell* **80,** 259–268.
2. Berridge, M. J. (1997) *J. Physiol. (London)* **499,** 291–306.
3. Kohn, E. C. & Liotta, L. A. (1995) *Cancer Res.* **55,** 1856–1862.
4. Hoenderop, J. G., van der Kemp, A. W., Hartog, A., van de Graaf, S. F., Van Os, C.H.,Willems, P. H. & Bindels, R. J. (1999) *J. Biol. Chem.* **274,** 8375–8378.
5. Peng, J. B., Chen, X. Z., Berger, U. V., Vassilev, P. M., Tsukaguchi, H., Brown, E. M. & Hediger, M. A. (1999) *J. Biol. Chem.* **274,** 22739–22746.
6. Kiselyov, K., Xu, X., Mozhayeva, G., Kuo, T., Pessah, I., Mignery, G., Zhu, X., Birnbaumer, L. & Muallem, S. (1998) *Nature (London)* **396,** 478–482.
7. Philipp, S., Cavalie, A., Freichel, M., Wissenbach, U., Zimmer, S., Trost, C., Marquart, A., Murakami, M. & Flockerzi, V. (1996) *EMBO J.* **15,** 6166–6171.

8. Vennekens, R., Hoenderop, J. G., Prenen, J., Stuiver, M., Willems, P. H., Droogmans, G., Nilius, B. & Bindels, R. J. (2000) *J. Biol. Chem.* **275,** 3963–3969.
9. Wissenbach, U., Niemeyer, B., Fixemer, T., Schneidewind, A., Trost, C., Cavalie, A., Reuss, K., Meese, E., Bonkhoff, H. & Flockerzi, V. (2001) *J. Biol. Chem*. **276,** in press.
10. Peng, J-B., Chen, X-Z., Berger, U. V., Weremowicz, S., Morton, C. C., Vassilev, P. M., Brown, E. M. & Hediger, M. A. (2000) *Biochem. Biophys. Res. Commun.* **278,** 326–332.
11. Scott., K. & Zuker, C. (1998) *Curr. Opin. Neurobiol.* **8,** 383–388.
12. Montell, C. (1997) *Mol. Pharmacol.* **52,** 755–763.
13. Hofmann, T., Schaefer, M., Schultz, G. & Gudermann, T. (2000) *J. Mol. Med.* **78,** 14–25.
14. Bertrand, B., Wakabayashi, S., Ikeda, T., Pouyssegur, J. & Shigekawa, M. (1994) *J. Biol. Chem.* **269,** 13703–13709.
15. Levitan, I. B. (1999) *Neuron* **22,** 645–648.
16. Erickson-Viitanen, S. & DeGrado, W. F. (1987) *Methods Enzymol.* **139,** 455–478.
17. Nishikawa, K., Toker, A., Johannes, F. J., Songyang, Z. & Cantley, L. C. (1997) *J. Biol. Chem.* **272,** 952–960.
18. Newton, A. C. (1995) *J. Biol. Chem.* **270,** 28495–28498.
19. Nishizuka, Y. (1995) *FASEB J.* **9,** 484–496.
20. Carafoli, E. & Klee, C. (1999) *Calcium as a Cellular Receptor* (Oxford Univ. Press, New York).
21. Zuhlke, R. D., Pitt, G. S., Deisseroth, K., Tsien, R. W. & Reuter, H. (1999) *Nature (London)* **399,** 159–162.
22. Ehlers, M. D., Zhang, S., Bernhadt, J. P. & Huganir, R. L. (1996) *Cell* **84,** 745–755.
23. Scott, K., Sun, Y., Beckingham, K. & Zuker, C. S. (1997) *Cell* **91,** 375–383.
24. Fanger, C. M., Ghanshani, S., Logsdon, N. J., Rauer, H., Kalman, K., Zhou, J., Beckingham, K., Chandy, K. G., Cahalan, M. D. & Aiyar, J. (1999) *J. Biol. Chem.* **274,** 5746–5754.
25. Xia, X. M., Fakler, B., Rivard, A., Wayman, G., Johnson-Pais, T., Keen, J. E., Ishii, T., Hirschberg, B., Bond, C. T., Lutsenko, S., *et al.* (1998) *Nature (London)* **395,** 503–507.
26. Nilius, B., Vennekens, R., Prenen, J., Hoenderop, J. G., Droogmans, G. & Bindels, R. M. (2001) *J. Biol. Chem.* **276,** 1020–1025.
27. Nilius, B., Vennekens, R., Prenen, J., Hoenderop, J. G., Bindels, R. J. & Droogmans, G. (2000) *J. Physiol. (London)* **527,** 239–248.
28. Chakravarthy, B., Morley, P. & Whitfield, J. (1999) *Trends Neurosci.* **22,** 12–16.
29. Warr, C. G. & Kelly, L. E. (1996) *Biochem. J.* **314,** 497–503.
30. Keranen, L. M. & Newton, A. C. (1997) *J. Biol. Chem.* **272,** 25959–25967.
31. Blobe, G. C., Sachs, C. W., Khan, W. A., Fabbro, D., Stabel, S., Wetsel, W. C., Obeid, L. M., Fine, R. L. & Hannun, Y. A. (1993) *J. Biol. Chem.* **268,** 658–664.